nature structural & molecular biology

A conserved PUF–Ago–eEF1A complex attenuates translation elongation

Kyle Friend[1], Zachary T Campbell[1], Amy Cooke[1,2], Peggy Kroll-Conner[3], Marvin P Wickens[1,2] & Judith Kimble[1–3]

PUF (Pumilio/FBF) RNA-binding proteins and Argonaute (Ago) miRNA-binding proteins regulate mRNAs post-transcriptionally, each acting through similar, yet distinct, mechanisms. Here, we report that PUF and Ago proteins can also function together in a complex with a core translation elongation factor, eEF1A, to repress translation elongation. Both nematode *(Caenorhabditis elegans)* and mammalian PUF–Ago–eEF1A complexes were identified, using coimmunoprecipitation and recombinant protein assays. Nematode CSR-1 (Ago) promoted repression of FBF (PUF) target mRNAs in *in vivo* assays, and the FBF-1–CSR-1 heterodimer inhibited EFT-3 (eEF1A) GTPase activity *in vitro*. Mammalian PUM2–Ago–eEF1A inhibited translation of nonadenylated and polyadenylated reporter mRNAs *in vitro*. This repression occurred after translation initiation and led to ribosome accumulation within the open reading frame, roughly at the site where the nascent polypeptide emerged from the ribosomal exit tunnel. Together, these data suggest that a conserved PUF–Ago–eEF1A complex attenuates translation elongation.

Translational regulation affects metazoan development, learning and human disease[1–3]. Of the many RNA-binding proteins regulating mRNA stability, localization and translation, the two classes relevant to this work are the PUF and Ago families. PUF proteins regulate a broad spectrum of mRNAs to maintain stem cells, among other functions[1,2]. Ago proteins bind small RNAs, most notably miRNAs, and act in many biological contexts, including in stem cells (reviewed in ref. 3).

PUF proteins regulate mRNA expression in virtually all eukaryotes[4]. One conserved mechanism, which has been established for *Saccharomyces cerevisiae*, *Caenorhabditis elegans* and human PUF proteins, relies on the direct recruitment of the Ccr4–Not deadenylase complex to target mRNAs, resulting in a shorter poly(A) tail length and either mRNA instability or translational repression[5,6]. PUF proteins in yeast and flies also use deadenylation-independent mechanisms, although the specifics of these mechanisms remain mostly unknown[7,8].

Ago proteins function within the miRISC complex to control target mRNA stability and translation. This complex controls deadenylation and stability of its target mRNAs[9–11], but its mechanism to control translation has garnered controversy. Best documented is its regulation of translation initiation[9–13]. However, a mechanism affecting translation elongation also appears to exist, as target mRNAs can be bound to polyribosomes[14]. One model is that miRISC promotes ribosomal drop-off during translation elongation[15]. Yet the specific mechanism by which miRISC, and hence Ago family members, inhibits translation elongation is not understood.

Here, we report that PUF and Ago proteins form an inhibitory complex with eEF1A, a GTPase required for translation elongation. FBF-1 (a *C. elegans* PUF protein) binds CSR-1 (a *C. elegans* Ago family member) *in vitro* and *in vivo*, and *csr-1* depletion leads to increased expression of FBF target mRNAs. The FBF-1–CSR-1 heterodimer forms a complex with EFT-3 (*C. elegans* eEF1A), and this FBF-1–CSR-1–EFT-3 ternary complex has inhibited GTPase activity. Notably, the PUF–Ago–eEF1A complex is conserved: human PUM2 (a PUF protein) associates with human AGO proteins *in vivo* and with eEF1A. Wild-type human PUM2 inhibits translation of both nonadenylated and polyadenylated mRNAs in rabbit reticulocyte lysate; however, PUM2 mutants that cannot form the PUM2–Ago–eEF1A complex or that cannot bind RNA are severely compromised for translation repression. Mechanistically, PUM2–Ago–eEF1A represses translation during elongation, with ribosomes accumulating ~100–140 nucleotides (nt) after the AUG within the open reading frame (ORF). We propose a model in which PUF and AGO proteins form a complex with eEF1A to inhibit its GTPase activity and attenuate translation elongation.

RESULTS

Association of *C. elegans* FBF-1 and CSR-1

To explore the molecular mechanisms of PUF protein function, we sought proteins that interact with two nearly identical *C. elegans* PUF proteins, FBF-1 and FBF-2, known collectively as FBF[16]. Previous yeast two-hybrid screens identified several FBF partners but no components of the translation machinery[17,18]. Here, we used recombinant, full-length GST–FBF-1 and GST–FBF-2 to select proteins from *C. elegans* lysates and to identify interacting proteins by mass spectrometry (**Supplementary Fig. 1** and **Supplementary Table 1**). Known FBF-interacting proteins, CPB-1 and NOS-3 (refs. 17,18), were detected in

[1]Department of Biochemistry, University of Wisconsin-Madison, Madison, Wisconsin, USA. [2]Graduate Program in Cellular and Molecular Biology, University of Wisconsin-Madison, Madison, Wisconsin, USA. [3]Howard Hughes Medical Institute, University of Wisconsin-Madison, Madison, Wisconsin, USA. Correspondence should be addressed to J.K. (jekimble@wisc.edu).

Received 18 July 2011; accepted 24 November 2011; published online 8 January 2012; doi:10.1038/nsmb.2214

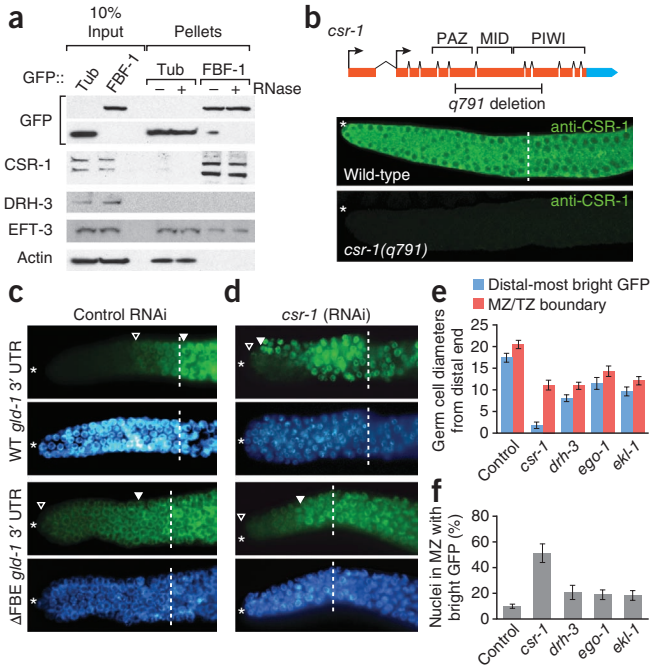

Figure 1 FBF-1 binds CSR-1 to repress target mRNA. (**a**) FBF-1 coimmunoprecipitates with CSR-1. Transgenic GFP::FBF-1 (FBF-1) was immunoprecipitated from adult hermaphrodites with or without RNase. Bound proteins (pellets) were probed on western blots for indicated proteins. CSR-1 and EFT-3 were both detected in FBF-1 immunoprecipitations, whereas DRH-3 and actin were not. Two CSR-1 isoforms exist *in vivo*[20,23], and both coimmunoprecipitate with FBF-1. CSR-1 did not coimmunoprecipitate with GFP::tubulin (Tub). (**b**) CSR-1 is expressed in the mitotic zone. Top, diagram of *csr-1* locus. The *q791* deletion removes crucial domains, resulting in a frameshift. Arrows, alternative promoter elements. Bottom: CSR-1 antibody[23] stains the wild-type mitotic zone cytoplasm (*, distal end of the gonad; dashed line, mitotic zone–transition zone boundary), but not in a *csr-1* mutant. (**c**,**d**) Adult germ lines expressing GFP::H2B (green) under control of wild-type (WT) or FBE-lacking (ΔFBE) *gld-1* 3′ UTR; nuclei seen with DAPI (blue). Marked include: *, distal end; open triangle, distal-most GFP-positive cell; closed triangle, distal-most bright GFP; dashed line, mitotic zone–transition zone boundary. Control RNAi, empty vector. GFP::H2B is normally repressed in distal region (top panels), but expands into distal germ cells without FBEs (lower panels) (**c**). *csr-1*(RNAi). GFP::H2B expanded more distally than control in panel **c** when reporter harbors an FBE (**d**). (**e**) GFP::H2B extent after RNAi against genes indicated, scoring only sterile animals to ensure effective RNAi. Blue columns, most distal germ-cell row with GFP::H2B-positive cell; red columns, mitotic zone–transition zone boundary. Error bars represent s.d. ($n > 30$). (**f**) Percent cells in mitotic zone with bright GFP::H2B.

addition to previously unknown putative partners CSR-1, one of 27 *C. elegans* Ago family members[19,20], and EFT-3, the *C. elegans* homolog of translation elongation factor 1A, eEF1A[21].

To directly test whether FBF-1 interacts with CSR-1 and EFT-3 *in vivo*, we immunoprecipitated tagged FBF-1 (ref. 22) from *C. elegans* lysate and probed for associated proteins. CSR-1 was specifically enriched, and this interaction was RNA-independent (**Fig. 1a**), indicating that FBF-1 and CSR-1 form a protein complex. By contrast, Dicer-related helicase (DRH-3), which is required to produce the 22-nt RNAs bound by CSR-1 (refs. 23,24), did not coimmunoprecipitate with FBF-1 (**Fig. 1a**), demonstrating that FBF-1 specifically binds CSR-1. EFT-3 was present in both FBF-1 and control coimmunoprecipitations (**Fig. 1a**), so we carried out further assays to confirm specificity of binding (see below). Our coimmunoprecipitation experiments suggested that CSR-1 should be expressed in the same germline region as FBF. FBF is enriched in the germ-cell cytoplasm at the distal end of the gonad[25], and we found CSR-1 in the same location (**Fig. 1b**), in addition to its known location in the proximal germ line[20]. Because FBF-1 and CSR-1 coimmunoprecipitate and are expressed in the same region, FBF-1 and CSR-1 probably interact *in vivo*.

CSR-1 promotes repression of FBF target mRNAs

PUF and Ago family members both repress translation[4,10], and models have suggested that miRNA binding sites proximal to PUF mRNA target sites may indicate an interaction[26]. To ask if FBF and CSR-1 might function together, we examined expression of an FBF reporter mRNA after CSR-1 depletion. In the reporter mRNA, the 3′ UTR of *gld-1*, an FBF target mRNA[25], was linked to an ORF encoding a GFP histone H2B fusion protein (GFP::H2B), which labels nuclei. We used RNAi to deplete *csr-1* from animals transgenic for reporters with either the wild-type *gld-1* 3′ UTR (WT *gld-1* 3′ UTR) or a mutant *gld-1* 3′ UTR (ΔFBE *gld-1* 3′ UTR) without FBF binding elements (FBEs)[27]. Briefly, fourth-stage larvae were treated by feeding RNAi, and the GFP::H2B reporter was scored one generation later in adult progeny. In control animals not depleted for CSR-1, GFP::H2B was absent from the distal-most germ cells with the WT *gld-1* 3′ UTR reporter (**Fig. 1c**, top panels), but GFP::H2B extended to the distal end in animals with the ΔFBE *gld-1* 3′ UTR reporter (**Fig. 1c**, bottom panels), as seen previously[27]. After CSR-1 depletion in animals carrying the WT *gld-1* 3′ UTR reporter, bright GFP::H2B expression was always shifted distally compared to controls ($n = 31/31$) (**Fig. 1d**, top panels) and was often in distal-most germ cells ($n = 12/31$). By contrast, *csr-1* RNAi had little effect on expression of the ΔFBE *gld-1* 3′ UTR reporter (**Fig. 1d**, bottom panels). As a control, the same reporter assay was used after proteins thought to form a complex with CSR-1 (ref. 24) were depleted, but these depletions did not affect the WT *gld-1* 3′ UTR reporter (**Fig. 1e**,**f**). Because total loss of FBE-mediated repression always leads to bright GFP::H2B in the distal-most germ cells[28], *csr-1* depletion does not completely eliminate FBE-mediated repression but instead severely compromises that repression. We conclude that CSR-1 reduces expression of FBF reporter mRNA and that this effect requires FBEs.

To validate our findings with the *gld-1* reporter mRNAs, we assayed two FBF target mRNAs, *gld-1* (ref. 25) and *cye-1* (ref. 29) mRNAs, in a *csr-1* mutant. GLD-1 protein is normally expressed at a low but graded level in the mitotic zone (**Supplementary Fig. 2a**, top panel), whereas CYE-1 is more uniform in the mitotic zone (**Supplementary Fig. 2a**, middle panel). In a *csr-1* deletion mutant, GLD-1 and CSR-1 both increased markedly in the mitotic zone, though GLD-1 was still graded (**Supplementary Fig. 2b**, top and middle panels). For controls, we also analyzed GLD-1 and CYE-1 levels in mutants of *drh-3*, *ego-1* and *ekl-1*, which are thought to function jointly with *csr-1* (refs. 20,24,30). In these mutants, we observed more GLD-1 and CYE-1 than wild-type, but not to the high level typical of *csr-1* mutants (**Supplementary Fig. 2c–e**). Therefore, wild-type CSR-1 lowers expression of at least two FBF target mRNAs.

These experiments suggest that FBF functions with CSR-1 to repress target mRNAs. Yet, the documented germline defects in *fbf* and *csr-1* mutants differ in many respects. The *fbf-1 fbf-2* double mutant germ lines are defective for germline self-renewal and hence have no mitotic zone[25] whereas *csr-1* is defective for chromosome segregation and embryonic viability[19]. We examined *csr-1* deletion mutants for mitotic zone defects and found the *csr-1* mitotic zone to be present but smaller than normal (**Supplementary Fig. 2b**). The reduced *csr-1* mitotic

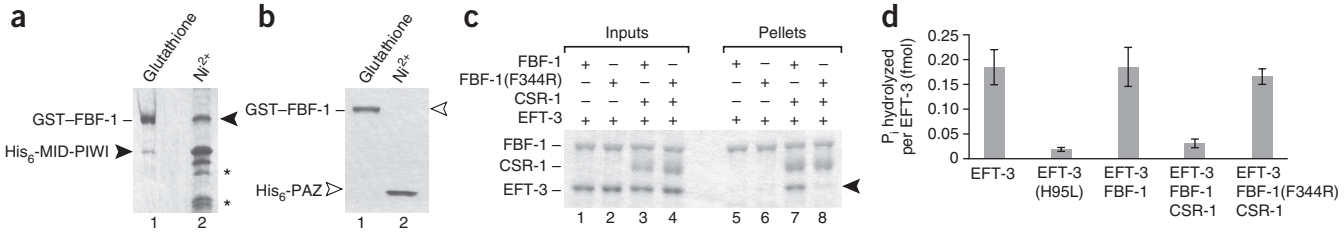

Figure 2 FBF-1–CSR-1–EFT-3 ternary complex formation reduces EFT-3 GTPase activity. (**a**) GST–FBF-1 and His_6-CSR-1(MID-PIWI) were coexpressed in the pETDuet system. Affinity selection was carried out with either glutathione to select GST–FBF-1 or Ni^{2+} to select His_6-MID-PIWI, respectively. GST–FBF-1 and His_6-MID-PIWI associate. His_6-MID-PIWI degradation products are indicated (*). (**b**) As in panel **a**, but GST–FBF-1 was coexpressed with CSR-1 PAZ (His_6-PAZ). FBF-1 and His_6-PAZ do not associate. (**c**) EFT-3 binds the FBF-1–CSR-1 complex. Recombinant EFT-3 was added to wild-type FBF-1, FBF-1(F344R), FBF-1–CSR-1 or FBF-1(F344R)–CSR-1 prepared from bacteria (inputs, 25% loaded). Glutathione was used to select GST–FBF-1 (wild-type and mutant) after incubation (pellets, 50% loaded). EFT-3 (arrowhead) specifically associated with wild-type FBF-1–CSR-1, but not with FBF-1 alone or with mutant FBF-1(F344R)–CSR-1. We note that the FBF-1–CSR-1–EFT-3 complex forms with apparent 1:1:1 stoichiometry. CSR-1 refers to His_6-CSR-1(MID-PIWI); FBF-1 refers to GST–FBF-1. (**d**) FBF-1–CSR-1 specifically inhibits EFT-3 GTPase activity. [γ-^{32}P]GTP was incubated with EFT-3, catalytically dead EFT-3(H95L), EFT-3 and FBF-1, EFT-3–FBF-1–CSR-1 or EFT-3 and FBF-1(F344R)–CSR-1. Liberated $^{32}P_i$ was counted after phase extraction. Error bars represent s.d. ($n = 3$).

zone is consistent with a functional overlap with FBF, but its presence demonstrates that CSR-1 is not required for all FBF functions. We suggest that CSR-1 and FBF can work together to repress mRNA expression through FBEs, but that they can also work independently. The independent functions probably involve interactions with other paralogs (for example, FBF with other Agos and CSR-1 with other PUFs) as well as interactions with other complexes (for example, FBF with Ccr4–Not deadenylase and CSR-1 with RISC).

FBF-1 interacts with the CSR-1 MID-PIWI domains

To directly assay FBF-1 interactions with CSR-1, we conducted biochemical analyses with purified recombinant proteins. Initially, we explored the interaction, focusing on conserved domains—the PUF repeats of FBF-1 (hereafter called FBF-1) and the MID-PIWI or PAZ domains of CSR-1. GST–FBF-1 (residues 121–612) was coexpressed with either His_6-MID-PIWI (residues 557–993) or His_6-PAZ (residues 378–505) in the pETDuet system, which allows simultaneous expression of multiple proteins. Affinity selection for GST–FBF-1 enriched His_6-MID-PIWI (**Fig. 2a**, lane 1) but not His_6-PAZ (**Fig. 2b**, lane 1); the reciprocal selection for His_6-MID-PIWI enriched GST–FBF-1 (**Fig. 2a**, lane 2), but selection for His_6-PAZ did not enrich GST–FBF-1 (**Fig. 2b**, lane 2). Therefore, purified FBF-1 interacts specifically with the CSR-1 MID-PIWI domains but not with its PAZ domain. Our next experiments used the CSR-1 MID-PIWI region, referred to as CSR-1 for brevity.

FBF-1 and CSR-1 form a complex with EFT-3 (eEF1A)

This work identifies EFT-3 as a potential FBF-1 interactor (**Supplementary Table 1**), and work by others identified human eEF1A as a potential AGO1 and AGO2 interactor[31], although the interaction was not confirmed for either nematode or human components. We hypothesized that the FBF-1–CSR-1 heterodimer might form a ternary complex with the translation elongation factor EFT-3. To explore that idea, we purified FBF-1 alone, the FBF-1–CSR-1 heterodimer and EFT-3 alone (**Fig. 2c**, lanes 1–4); attempts to purify CSR-1 by itself were unsuccessful. FBF-1 alone did not bind EFT-3 (**Fig. 2c**, lane 5), but the FBF-1–CSR-1 heterodimer did bind EFT-3 (**Fig. 2c**, lane 7), suggesting the existence of a ternary complex. This ternary complex was observed in the absence of GTP (**Fig. 2c**, lane 7), but FBF-1–CSR-1 also bound EFT-3 when GTP was included (**Supplementary Fig. 3a**). We confirmed the identity of CSR-1 and EFT-3 proteins in these pull-down assays by western blotting (**Supplementary Fig. 3b**). We examined FBF-1 for conserved residues that are not involved in RNA-binding and found a broadly conserved phenylalanine residue (Phe344) (**Supplementary Fig. 3c**). We hypothesized that mutant FBF-1(F344R) might be defective for ternary complex formation. Although FBF-1(F344R) was able to bind CSR-1 (**Supplementary Fig. 3d**), the FBF-1(F344R)–CSR-1 heterodimer failed to bind EFT-3 (**Fig. 2c**, lane 8). We propose that FBF-1–CSR-1–EFT-3 exists as a complex.

The FBF-1–CSR-1 heterodimer inhibits EFT-3 GTPase activity

How might the complex affect translation? eEF1A family members possess GTPase activity, which is required during translation elongation in order to release aminoacyl-tRNAs upon delivery to the ribosome. Purified eEF1A has intrinsic GTPase activity, which is stimulated by ribosomes[32]. We hypothesized that the PUF–Ago complex might inhibit eEF1A activity because PUF and Ago proteins can inhibit translation[4,9–11]. To test this idea, we first confirmed that wild-type EFT-3 possesses GTPase activity compared to a catalytically dead mutant EFT-3(H95L)[33] (**Fig. 2d**; **Supplementary Fig. 3e**). We then assayed FBF-1 alone and the FBF-1–CSR-1 heterodimer for an effect on the EFT-3 GTPase activity. FBF-1 alone did not reduce GTPase activity, but the FBF-1–CSR-1 heterodimer reduced GTPase activity to a level similar to that of catalytically dead EFT-3(H95L) (**Fig. 2d**). Notably, the mutant FBF-1(F344R)–CSR-1 heterodimer, which did not form a complex with EFT-3, also did not inhibit EFT-3 GTPase activity (**Fig. 2d**). Inhibition of EFT-3 GTPase activity in the FBF-1–CSR-1–EFT-3 complex suggests that the complex may repress translational elongation.

A human PUM2–AGO–eEF1A complex

We predicted that a PUM2–AGO–eEF1A complex might also form in humans. Initially, we tested whether PUM2 binds AGO family members *in vivo*. HEK293T cells were transiently transfected with constructs encoding the Flag-tagged PUF repeats of human PUM2 (PUM2-3×Flag) and Flag-hemagglutinin (HA)-tagged, full-length human AGOs1–3 (ref. 31). Using anti-HA antibodies, AGOs1–3 were immunoprecipitated from cells cross-linked with formaldehyde under denaturing conditions with RNase to isolate endogenous complexes[34]. Anti-Flag western blots revealed that PUM2 and AGOs1–3 coimmunoprecipitate (**Supplementary Fig. 4a**). We confirmed that PUM2 coimmunoprecipitates with AGOs1–3 without cross-linking (**Supplementary Fig. 4b**). To test whether PUM2 is critical for the

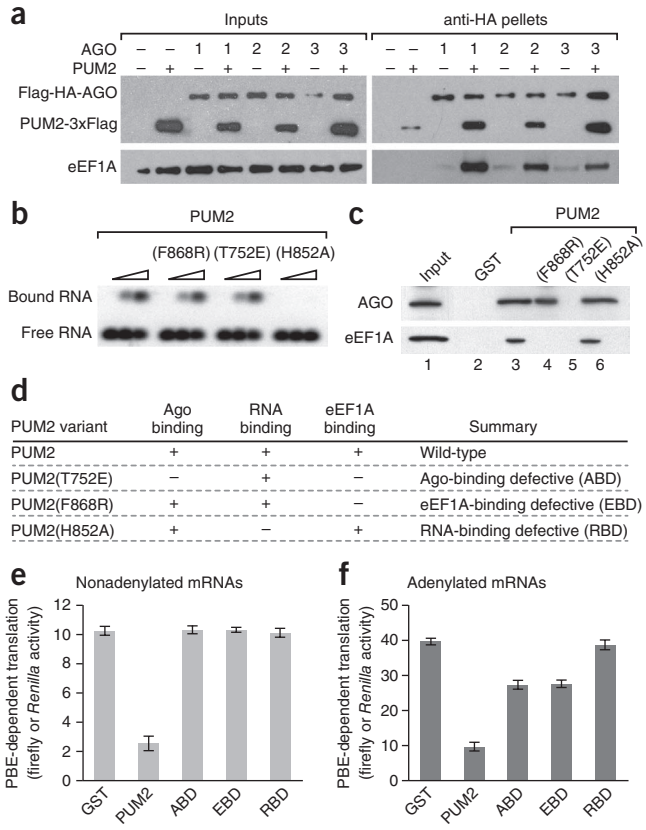

Figure 3 PUM2–Ago–eEF1A complex inhibits protein production. (**a**) Human PUM2 promotes eEF1A association with Ago. Western blots using Flag antibody to detect 3×Flag-PUM2 and Flag-HA-AGOs1–3 (top) or eEF1A antibody (bottom). PUM2 coexpression markedly enhanced eEF1A coimmunoprecipitation. (**b**) RNA binding by PUM2 variants. Recombinant PUM2, PUM2(F868R), PUM2(T752E) and PUM2(H852A) at increasing concentrations (triangle) were assayed for binding the *hunchback* PBE sequence. (**c**) Complex formation with PUM2 variants. AGO coprecipitates with all PUM2 mutants except PUM2(T752E). eEF1A coprecipitates with wild-type and PUM2(H852A) but not with PUM2(F868R) or PUM2(T752E). Equivalent amounts of recombinant PUM2 proteins were added to reticulocyte lysate (input) in the presence of RNase. (**d**) PUM2 variant summary. (**e**) PBE-dependent translation repression of nonadenylated reporter mRNA. Recombinant GST or GST-tagged PUM2 variants, nonadenylated firefly luciferase mRNA with 3× PBEs in its 3′ UTR and control nonadenylated *Renilla* luciferase reporter were added to reticulocyte lysate. To monitor PBE-dependent translation, firefly luciferase production was normalized to *Renilla* luciferase production. Only wild-type PUM2 inhibited translation of nonadenylated firefly luciferase mRNA. Note that protein output was not corrected for mRNA level, because all reaction mixtures contained the same initial quantity of reporter mRNAs, and wild-type PUM2 reaction mixtures had more final mRNA than others. Error bars represent s.d. ($n = 3$). (**f**) As in panel **e**, but with polyadenylated mRNAs.

association of Ago and eEF1A, we conducted the same transfection experiments as above in the presence or absence of PUM2. When PUM2 was coexpressed, AGO1–3 coimmunoprecipitations pulled down markedly more eEF1A than when PUM2 was omitted, suggesting that PUM2–AGO binds eEF1A *in vivo* (**Fig. 3a**). We conclude that the PUM2–AGO–eEF1A complex is conserved.

PUM2 mutants abolish complex formation

We turned to rabbit reticulocyte lysate to characterize PUM2–Ago–eEF1A effects on translation. For these experiments, we first identified PUM2 mutants that abolish complex formation or RNA binding. Each PUM2 variant tested was composed of the PUF repeats of human PUM2 (residues 706–1062) and was generated as a GST–PUM2 fusion protein. PUM2 refers to the wild-type version; PUM2(F868R) alters the conserved phenyalanine corresponding to FBF-1(F344); PUM2(T752E) changes a conserved threonine residue (**Supplementary Fig. 5a–c**); and PUM2(H852A) was predicted to abrogate RNA binding[35]. Of these four proteins (**Supplementary Fig. 5d**), only PUM2(H852A) failed to bind an RNA carrying PUF-binding elements (PBEs) (**Fig. 3b**). When assayed for complex formation, wild-type PUM2 and PUM2(H852A) coprecipitated Ago and eEF1A from rabbit reticulocyte lysate (**Fig. 3c**, lanes 3 and 6). PUM2(F868R) bound Ago, but not eEF1A (**Fig. 3c**, lane 4), and PUM2(T752E) failed to bind either Ago or eEF1A (**Fig. 3c**, lane 5). In summary, PUM2(T752E) is Ago-binding defective (ABD); PUM2(F868R) is eEF1A-binding defective (EBD); and PUM2(H852A) is RNA-binding defective (RBD) but binds both Ago and eEF1A (**Fig. 3d**). The PUM2–Ago heterodimer recruits eEF1A, and PUM2 RNA-binding activity is not required for complex formation.

PUM2–Ago–eEF1A represses mRNA translation

To assay effects of the PUM2–Ago–eEF1A complex on translation, we used reporter mRNAs in reticulocyte lysate. We first quantitated Ago levels in the lysate (**Supplementary Fig. 6a**) and added an equivalent amount of PUM2. To ensure that reticulocyte lysate was not limiting for translation, we titrated mRNA encoding firefly luciferase with 3× PBEs in its 3′ UTR (PBEs bind human PUM1 and PUM2 (refs. 36,37)) against constant control *Renilla* luciferase reporter lacking PBEs (**Supplementary Fig. 6b**). PUM2 did not destabilize reporter mRNAs; in fact, PUM2 stabilized them (**Supplementary Fig. 6c**). Therefore, the ratio of firefly to *Renilla* luciferase enzyme activities allows us to monitor PBE-dependent translation. We first assayed nonadenylated mRNA (**Fig. 3e**) to exclude from our analysis PUF-mediated deadenylation effects[5]. Wild-type PUM2 inhibited mRNA translation, but the three mutant PUM2 proteins failed to repress reporter expression (**Fig. 3e**). Most notably, the ABD and EBD mutants, which disrupt PUF–Ago–eEF1A complex formation (**Fig. 3b**), did not repress the reporter.

Most natural mRNAs are polyadenylated, so we also assayed polyadenylated reporter mRNAs (**Fig. 3f**). Similar to the effects observed on the nonadenylated reporter mRNA, wild-type PUM2 repressed translation of polyadenylated mRNA whereas PUM2(RBD) did not. Notably, the PUM2 ABD and EBD mutants remained capable of limited repression. One possibility might have been that the ABD and EBD mutants had this minor effect by promoting mRNA deadenylation. However, mRNA adenylation was unaffected in our assays (**Supplementary Fig. 6d**). An open question is how PUM2(ABD and EBD) mutants repress the polyadenylated reporter in the absence of both deadenylation and PUM2–Ago–eEF1A complex formation. Indeed, these mutants suggest the existence of yet another mechanism of PUF repression. Because PUF proteins associate with the protein nanos[38], we considered the possibility that the region of PUM2 important for its nanos association might be important for PUM2 repression. However, PUM2(G987D) repressed both nonadenylated and polyadenylated reporter mRNAs as well as wild-type PUM2 (**Supplementary Fig. 7**). Together, results from experiments using nonadenylated and polyadenylated mRNA reporters suggest that the PUF–Ago–eEF1A complex represses translation and that it does so independent of mRNA deadenylation.

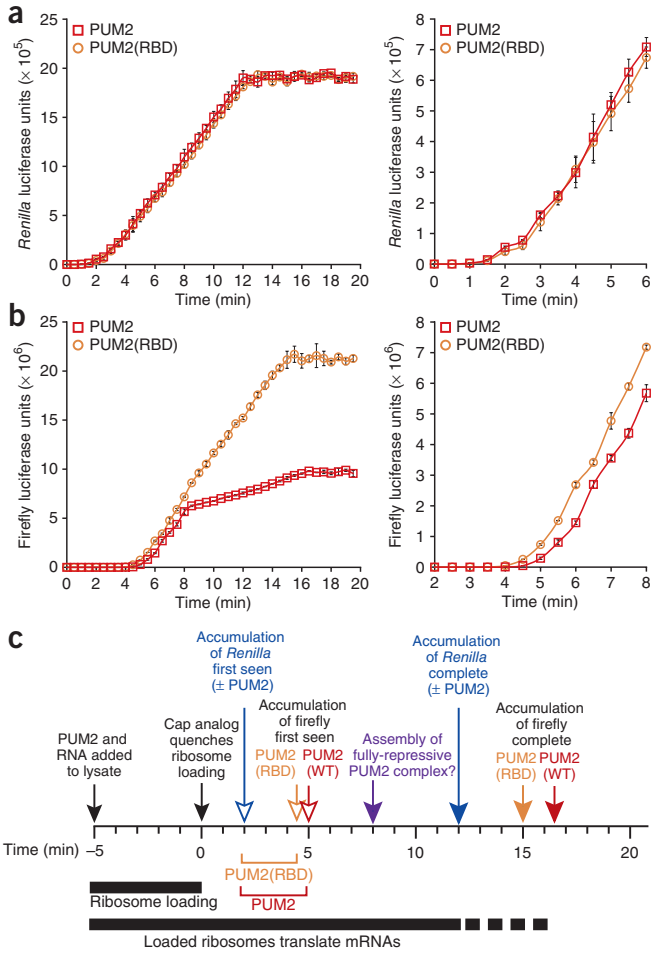

Figure 4 Kinetics of PUM2 translational repression. (**a**,**b**) PUM2 proteins were incubated with reporter mRNAs in reticulocyte lysate for 5 min to ensure ribosome loading; at time $t = 0$, excess mRNA cap analog was added to inhibit *de novo* 40S ribosomal subunit loading. Luciferase production was monitored every 30 seconds. Error bars represent s.d. ($n = 3$). (**a**) *Renilla* luciferase production. Left, kinetics of *Renilla* luciferase production were equivalent for PUM2 and PUM2(RBD); right, enlargement of early time points. (**b**) Firefly luciferase production. Left, firefly luciferase production was delayed with PUM2 compared to PUM2(RBD) and markedly inhibited midway through the reaction. The PUM2 curve was similar to that of PUM2(RBD) from the ~5- to 8-min time points (albeit with a 30-s delay), suggesting that a fully functional repressive complex forms slowly. Right, enlargement of data points when firefly luciferase is first produced. (**c**) To estimate translational elongation rate, we compared the time required to first produce either firefly or *Renilla* luciferase (firefly luciferase is 319 residues longer than *Renilla* luciferase). In reaction mixtures with PUM2(RBD), the first firefly luciferase protein was detected 2.5 min after the first *Renilla* luciferase (4.5 min for firefly versus 2 min for *Renilla*). From this difference, we infer an estimated translational elongation rate (eTER) of 2.12 residues per second (319/150 residues s^{-1}). In reaction mixtures with wild-type PUM2, the same calculation yields an eTER of 1.77 residues per second. This modest decrease was seen at a time well before PUM2 became fully repressive (8 min after cap analog addition). Therefore, PUM2 may affect translation elongation by using multiple mechanisms.

PUM2–Ago–eEF1A represses translation after initiation

We next investigated the mechanism of PUM2 translation inhibition, again in rabbit reticulocyte lysates. Initially, we carried out a standard assay for inhibition of translation initiation: we fractionated polyribosomes to ask if PUM2 inhibits the association of its target mRNA with ribosomes. *In vitro* translation reaction experiments were conducted as above with firefly mRNA (3× PBEs) and *Renilla* mRNA (control) in the presence of PUM2 or PUM2(RBD). Reaction mixtures were quenched with cycloheximide (maintains ribosomes on mRNA) or puromycin (removes ribosomes from mRNA) and separated over a sucrose gradient. After centrifugation, polyribosome profiles were indistinguishable when PUM2 or PUM2(RBD) was added, although puromycin did disrupt polyribosomes (**Supplementary Fig. 8a**,**b**). Moreover, by northern blots, the 3×PBE-containing mRNA associated with polyribosomes to the same level as the control mRNA, if either PUM2 or PUM2(RBD) was added (**Supplementary Fig. 8c**). As the 3×PBE-containing mRNA migrated in lighter fractions after puromycin addition, it is bound to ribosomes (**Supplementary Fig. 8d**). Although these data contrast observations that miRNA-mediated translation repression occurs at initiation in rabbit reticulocyte lysate[39], we note that we investigated PUF–Ago–eEF1A, not miRNAs. Therefore, ribosomal association with PUM2-bound mRNA appears unaffected by this assay, leading us to ask further questions about how translation is inhibited.

We next varied the translation assays to ask if PUM2-mediated repression occurs after translation initiation. Reporter RNAs plus purified recombinant PUM2 protein were incubated in lysate for 5 min to begin translation; then excess mRNA cap analog was added to quench additional ribosomal loading and thus to block translation initiation. Production of firefly (which is subject to PUM2 regulation) and *Renilla* luciferase was monitored in the presence of either PUM2 or PUM2(RBD) over time. In the absence of the cap analog, reporters produced luciferase linearly for about 45 min; however, in the presence of the cap analog, luciferase production stopped much earlier. The control *Renilla* luciferase RNA plateaued after only ~13 min in the presence of either PUM2 or PUM2(RBD) (**Fig. 4a**). This early plateau indicated that the excess cap analog had abolished *de novo* 40S ribosomal subunit loading. With the RNA-binding defective PUM2 variant, expression from the firefly luciferase mRNA plateaued after ~15 min, a bit after the *Renilla* control, presumably because the firefly luciferase protein product is larger. However, wild-type PUM2 had a marked effect on firefly luciferase expression, decreasing sharply after only 8 min (**Fig. 4b**, left panel), an effect that can account for the difference in synthesized protein shown in **Figure 3e**,**f**. Wild-type PUM2 also modestly, but reproducibly, delayed the initial production of firefly luciferase relative to PUM2(RBD), an effect that probably reflects slower translation elongation (**Fig. 4b**, right panel; summarized in **Fig. 4c**). The slowed translation elongation is consistent with inhibited eEF1A GTPase activity in the PUM2–Ago–eEF1A complex, but the effect was not large enough to account for the 75% reduction in the quantity of synthesized protein (**Fig. 3e**,**f**). We conclude that PUM2 slows translation elongation and blocks protein production from its target mRNA.

PUM2–Ago–eEF1A attenuates translation elongation

We considered possible mechanisms by which PUM2 might inhibit protein production: it might attenuate translation elongation, consistent with the ribosome drop-off model proposed for miRNA-mediated translation repression[15]; it might inhibit translation termination; or it might promote destruction of nascent polypeptides during translation, as observed for miRNA-mediated repression[40]. The first two mechanisms make predictions about effects on ribosome position. If ribosomes drop off the mRNA during elongation, ribosomal density should be higher at the 5′ end of the ORF and taper off toward the 3′ end. If translation termination is inhibited, ribosomes should

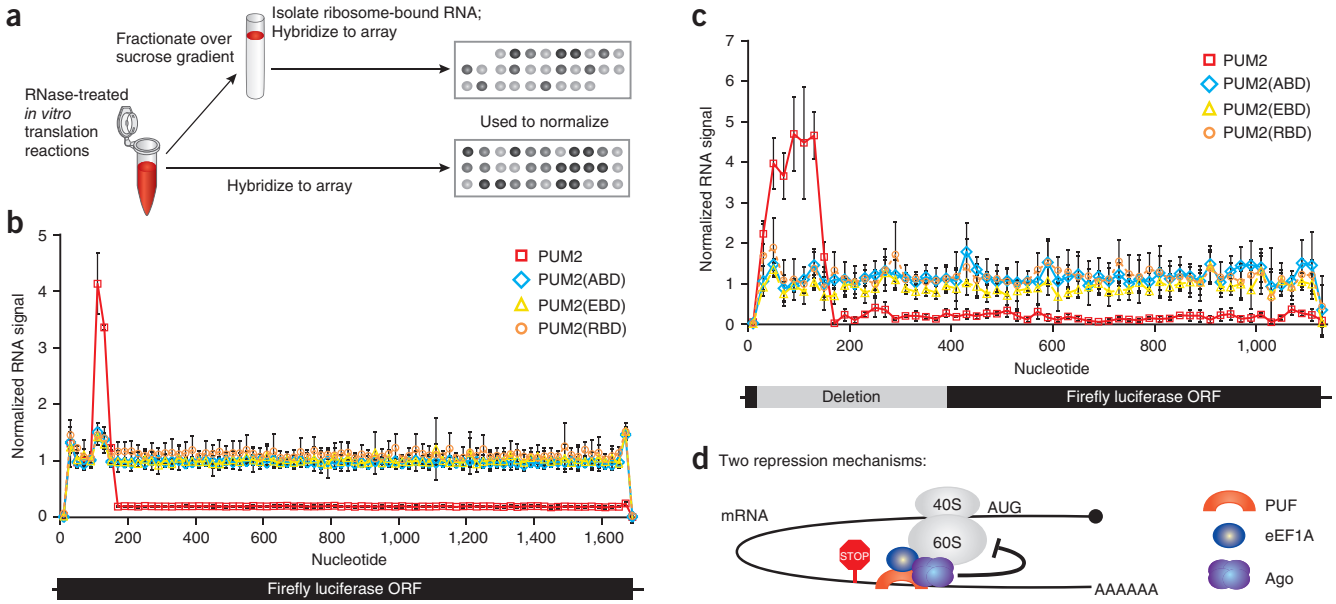

Figure 5 Human PUM2 attenuates translation elongation. (**a**) Ribosomal footprinting protocol. *In vitro* translation reaction experiments were conducted with radiolabeled firefly luciferase mRNA harboring 3× PBEs, and reactions were quenched with cycloheximide and treated with RNase. RNA from monoribosome fractions was collected and hybridized to a spotted array with oligonucleotides complementary to firefly mRNA. Signals from monoribosome-bound RNA fragments were normalized with input RNA fragments. (**b**) PUM2 affects ribosome position. PUM2, PUM2(ABD), PUM2(EBD) or PUM2(RBD) were added to reticulocyte lysate, and ribosomal footprinting was carried out as diagrammed in panel **a**. At the 5′ end of the ORF, ribosomal density is equivalent for all samples, a level that continues across the ORF when PUM2(ABD, EBD and RBD) mutants are added. With wild-type PUM2, ribosomal density peaks at ~100–140 nt and decreases to a level lower than that seen with PUM2 mutants. Therefore, translation is attenuated during elongation. Note that samples with wild-type PUM2 had more input RNA signal, owing to stabilized mRNA (**Supplementary Fig. 6b**), which dampens the signal observed for ribosomal footprints, once normalized. Error bars represent s.d. ($n = 3$). (**c**) As in panel **b**, but footprinting was carried out with a mutant firefly luciferase mRNA with ~500 nucleotides removed after the start codon (grey). As above, wild-type PUM2 caused ribosomes to accumulate over the first ~40–140 nt. Ribosomal density again dropped after this site of accumulation to a level lower than that seen with the PUM2 mutants, which all had equivalent ribosomal density across the ORF. (**d**) Model for how the PUF–Ago–eEF1A complex attenuates translation elongation. See text for explanation.

accumulate at the 3′ end of the ORF. High-resolution ribosomal footprinting was previously described at a genomic level[41], and we modified this approach for our single mRNA reporter (**Fig. 5a**). Briefly, *in vitro* translation reaction experiments were carried out with radiolabeled firefly luciferase mRNA (with 3× PBEs). Reaction mixtures contained PUM2, PUM2(ABD), PUM2(EBD) or PUM2(RBD). Translation reaction mixtures were quenched with cycloheximide and treated with RNase One, then fractionated over a sucrose gradient to isolate ribosome-bound RNA fragments. These RNA fragments were extracted from the monoribosome peak and hybridized to a spotted array containing overlapping DNA oligonucleotides complementary to the firefly luciferase mRNA (**Supplementary Fig. 9**). RNA signals from monoribosome fractions were normalized to signal from unfractionated samples to control for hybridization efficiency, uridine content and RNase sensitivity and then plotted across the mRNA (**Fig. 5b**). We find it striking that in the presence of PUM2, a large peak occurs ~100–140 nt into the ORF, and then ribosomal footprints are sharply reduced across the remainder of the ORF. The peak coincides with the position at which nascent polypeptide should emerge from the ribosomal exit tunnel (~30–40 residues[42]). Importantly, the ribosomal footprints observed in samples with PUM2(ABD and EBD) were similar to that with PUM2(RBD). Therefore, the ribosomal footprinting profile is only altered when PUM2 can form a ternary complex on its target mRNA. To ensure that the observed ribosomal profile was independent of nucleotide sequence, we repeated our ribosomal footprinting experiment with firefly luciferase mRNA lacking ~500 nucleotides after the initiation codon (including the sequence where ribosomes accumulated above). Again, we observed decreased ribosomal density after the first ~140 nucleotides into the ORF only when wild-type PUM2 was added (**Fig. 5c**). We conclude that the PUM2–Ago–eEF1A complex attenuates translation elongation, causing ribosomes to accumulate within the ORF.

DISCUSSION

Our data support three main conclusions that advance our understanding of how PUF and Ago proteins regulate translation. First, PUF and Ago proteins can form a conserved complex containing the core translation elongation factor, eEF1A. Second, the nematode complex inhibits eEF1A GTPase activity, and the human complex represses translation. Third, the complex blocks elongation at a site ~100–140 nucleotides into the open reading frame, where the nascent peptide is expected to emerge from the ribosomal exit tunnel. Below, we discuss the implications of these findings and propose a model to describe our observations: that PUF–Ago inhibits eEF1A GTPase activity and blocks translation elongation.

A conserved PUF–Ago–eEF1A complex

Studies done prior to this work focused on either PUF or Ago proteins[4,9–11]. One hint that the two might work together was a bioinformatics analysis of human 3′ UTRs, revealing a nonrandom proximity of PUF protein binding elements and miRNA binding sites[26]. Here, we demonstrate not only that PUF and Ago proteins interact but also that the PUF–Ago heterodimer associates with eEF1A and inhibits its GTPase activity. Our focus in nematodes was the FBF-1 PUF protein

and the CSR-1 Ago protein, but we suspect that other PUF–Ago combinations may occur, as the nematode genome encodes 11 PUFs and 27 Agos. FBF-1 and CSR-1 are divergent members of their respective families, yet both proteins possess signature domains. Moreover, CSR-1 has slicing activity[23] despite its noncanonical function in chromosome segregation[19]. One possibility might have been that the FBF-1–CSR-1 association was atypical. However, in mammals, human PUM2 can associate with three AGOs (AGO1, AGO2 and AGO3), suggesting conservation. We suggest that multiple PUF–Ago combinations exist both in nematodes and mammals. A question for the future is whether individual PUFs and Agos behave differently with respect to their participation in the PUF–Ago–eEF1A complex.

Small RNAs cannot be essential for formation of the PUF–Ago–eEF1A complex. The MID-PIWI domain of Ago is sufficient to form the complex, and together with its PUF partner, the MID-PIWI domain inhibits eEF1A GTPase activity. Yet the MID-PIWI domain cannot bind small RNAs on its own. By contrast, the PAZ domain of Ago is not required to assemble the complex (**Fig. 2c**), but this PAZ domain drives small RNA loading[43]. Nonetheless, PUF–Ago–eEF1A complexes formed *in vivo* contain full-length Agos and probably associate with small RNAs. An attractive idea is that the PUF–Ago–eEF1A complex coordinates PUF and miRNA regulation.

The interaction between the PUF–Ago heterodimer and eEF1A complex is reminiscent of the original identification of Ago in a complex with eIF2 (ref. 44), which is structurally similar to eEF1A and also possesses GTPase activity. Moreover, two *Drosophila* RNA-binding proteins, dFXR and VIG, coordinate with Ago2 in the context of miRISC to repress target mRNAs[45]. A promising possibility is that Ago proteins can work with other RNA-binding proteins and other translation factors to modulate multiple steps of protein synthesis.

PUF–Ago–eEF1A regulates translation elongation

Figure 5d presents a model for how the PUF–Ago–eEF1A complex may control translation elongation. Central to this model is its anchor through the PUF–Ago heterodimer to regulatory elements in the 3′ UTR and its association with an inhibited core translation elongation factor, eEF1A. Also central to this model is a block within the ORF at a position corresponding roughly to where the nascent polypeptide emerges from the ribosomal exit tunnel. Our kinetic analysis of protein production from a PUM2-repressed reporter mRNA (**Fig. 4**) suggested two phases of translational inhibition. An initial modest inhibition was inferred from a slower elongation rate, consistent with inhibition of eEF1A GTPase activity; a subsequent full repression was inferred from a complete block in protein synthesis seen later. Full repression may require a conformational change in the PUF–Ago–eEF1A complex, require its modification, or require recruitment of additional factors. If ribosomes do indeed accumulate where the nascent polypeptide leaves the ribosomal exit tunnel, the existence of an additional factor that recognizes the nascent polypeptide seems likely.

The model in **Figure 5d** does not include any small RNA associated with Ago, because our work focused on Ago, PUF and eEF1A proteins, not small RNAs. For example, an miRNA binding site was not engineered into the reporter 3′ UTRs, and miRNAs were not added to the reaction mixtures. One possibility is that the PUF–Ago–eEF1A mechanism reveals a role for Ago that does not rely on small RNAs. Perhaps more likely is the idea that small RNAs influence recruitment, either in an essential or facilitating manner. Addressing the role of small RNAs in this mechanism is an obvious next step for future analyses.

Repression at the level of translation initiation is emerging as a favored mechanism of translational control by miRNAs[9–11]. We provide two lines of evidence that the PUF–Ago–eEF1A complex does not have a major effect on translation initiation. First, polyribosomal profiles were the same for a PUM2-repressed mRNA and a control mRNA (**Supplementary Fig. 8**). Second, the same initial slope was observed in our kinetic analysis of protein production by PUM2-repressed and control mRNAs (**Fig. 4**). In addition, PUM2 repression occurred in the presence of excess mRNA cap analog, suggesting that its repression is exerted after loading 40S ribosomal subunits. Although we cannot exclude the possibility of a minor effect on translation initiation, our results strongly point to translational elongation as the major level at which the PUF–Ago–eEF1A complex exerts its repressive effects.

How does the proposed PUF–Ago–eEF1A mechanism compare to established mechanisms of regulation at the level of translation elongation? Perhaps the best-known mechanism is that adopted by the signal recognition particle (SRP) during synthesis of membrane proteins[46], where translation elongation is inhibited[47] until SRP docks with the endoplasmic reticulum[46]. The PUF–Ago–eEF1A mechanism resembles this case in that ribosomes accumulate at a similar position within the ORF. However, no role for 3′ UTR binding proteins is known for the SRP block. Recently discovered is the hnRNP E1 association with eEF1A to inhibit translation elongation; however, hnRNP E1 does not inhibit eEF1A GTPase activity but instead inhibits eEF1A dissociation from the ribosome[48]. Another case is miRISC, which is thought to promote ribosomal drop-off from a targeted mRNA but not at a given position within the ORF[15]. Therefore no established mechanism fits the PUF–Ago–eEF1A model completely.

Why multiple PUF and Ago mechanisms?

The PUF–Ago–eEF1A mechanism controlling translation elongation (**Fig. 5d**) is not the only mechanism used by PUF and Ago proteins, and it is perhaps not even the primary mechanism. Its relative importance to other well-established mechanisms (for example, deadenylation and instability, see above) remains unknown. Why use multiple mechanisms? We do not know, but we have three suggestions. One is security: if the PUF protein or Ago protein fails to silence a target mRNA with one mechanism, the regulator may invoke a different mechanism to repress the escaped mRNA. A second idea is reversibility: destruction is a dead end for an mRNA, but blocked elongation might ensure robust activation at a later step. A third idea is subcellular compartmentalization: as an mRNA emerges from the nucleus, it meets one subcellular environment, but upon localization, for example to stress granules, the mRNA enters a different environment. Translational repression in (or localization to) distinct subcellular locales may differentially use one mechanism over another. Critical issues for the future include unraveling the biological functions, relationships and regulation of the various PUF and Ago mechanisms.

METHODS

Methods and any associated references are available in the online version of the paper at http://www.nature.com/nsmb/.

Note: Supplementary information is available on the Nature Structural & Molecular Biology website.

ACKNOWLEDGMENTS

We thank H. Tabara (Kyoto University) for providing CSR-1 and DRH-3 antibodies and E. Kipreos (University of Georgia) for the CYE-1 antibody. We thank Kimble and Wickens lab members for discussion; we also thank E. Lund and S. Kennedy for critical reading of the manuscript and A. Helsley-Marchbanks and L. Vanderploeg for help with the manuscript and figure preparation. Mass spectrometry was carried out with support from the Human Proteomics Program at the University of Wisconsin-Madison.

AUTHOR CONTRIBUTIONS
K.F. conducted the experiments with the exception of phylogenetic analysis (Z.T.C.), luciferase reporter mRNA production (A.C.) and *csr-1* mutant generation (P.K.-C.). K.F., M.P.W. and J.K. prepared the manuscript. K.F. is supported by PF-10-127-01-DDC from the American Cancer Society, Z.T.C. by US National Institutes of Health (NIH) postdoctoral fellowship F32 GM095169, A.C. by NIH training grant T32 GM07215 and an Advanced Opportunity Fellowship from the University of Wisconsin-Madison, M.P.W. by NIH grants GM031892 and GM050942 and J.K. by NIH grant GM069454. J.K. is an investigator of the Howard Hughes Medical Institute.

COMPETING FINANCIAL INTERESTS
The authors declare no competing financial interests.

Published online at http://www.nature.com/nsmb/.
Reprints and permissions information is available online at http://www.nature.com/reprints/index.html.

1. Thompson, B., Wickens, M. & Kimble, J. Translational control in development. in *Translational Control in Biology and Medicine* (eds. Mathews, M.B., Sonenberg, N. & Hershey, J.W.B.) 507–544 (Cold Spring Harbor Laboratory Press, Woodbury, New York, 2007).
2. Dubnau, J. *et al.* The *staufen/pumilio* pathway is involved in *Drosophila* long-term memory. *Curr. Biol.* **13**, 286–296 (2003).
3. Alvarez-Garcia, I. & Miska, E.A. MicroRNA functions in animal development and human disease. *Development* **132**, 4653–4662 (2005).
4. Wickens, M., Bernstein, D.S., Kimble, J. & Parker, R.A. PUF family portrait: 3′UTR regulation as a way of life. *Trends Genet.* **18**, 150–157 (2002).
5. Goldstrohm, A.C., Hook, B.A., Seay, D.J. & Wickens, M. PUF proteins bind Pop2p to regulate messenger mRNAs. *Nat. Struct. Mol. Biol.* **13**, 533–539 (2006).
6. Suh, N. *et al.* FBF and its dual control of *gld-1* expression in the *Caenorhabditis elegans* germline. *Genetics* **181**, 1249–1260 (2009).
7. Chagnovich, D. & Lehmann, R. Poly(A)-independent regulation of maternal *hunchback* translation in the *Drosophila* embryo. *Proc. Natl. Acad. Sci. USA* **98**, 11359–11364 (2001).
8. Hook, B.A., Goldstrohm, A.C., Seay, D.J. & Wickens, M. Two yeast PUF proteins negatively regulate a single mRNA. *J. Biol. Chem.* **282**, 15430–15438 (2007).
9. Djuranovic, S., Nahvi, A. & Green, R. A parsimonious model for gene regulation by miRNAs. *Science* **331**, 550–553 (2011).
10. Fabian, M.R., Sonenberg, N. & Filipowicz, W. Regulation of mRNA translation and stability by microRNAs. *Annu. Rev. Biochem.* **79**, 351–379 (2010).
11. Huntzinger, E. & Izaurralde, E. Gene silencing by microRNAs: contributions of translational repression and mRNA decay. *Nat. Rev. Genet.* **12**, 99–110 (2011).
12. Pillai, R.S. *et al.* Inhibition of translational initiation by Let-7 MicroRNA in human cells. *Science* **309**, 1573–1576 (2005).
13. Humphreys, D.T., Westman, B.J., Martin, D.I. & Preiss, T. MicroRNAs control translation initiation by inhibiting eukaryotic initiation factor 4E/cap and poly(A) tail function. *Proc. Natl. Acad. Sci. USA* **102**, 16961–16966 (2005).
14. Olsen, P.H. & Ambros, V. The *lin-4* regulatory RNA controls developmental timing in *Caenorhabditis elegans* by blocking LIN-14 protein synthesis after the initiation of translation. *Dev. Biol.* **216**, 671–680 (1999).
15. Petersen, C.P., Bordeleau, M.E., Pelletier, J. & Sharp, P.A. Short RNAs repress translation after initiation in mammalian cells. *Mol. Cell* **21**, 533–542 (2006).
16. Zhang, B. *et al.* A conserved RNA-binding protein that regulates sexual fates in the *C. elegans* hermaphrodite germ line. *Nature* **390**, 477–484 (1997).
17. Luitjens, C., Gallegos, M., Kraemer, B., Kimble, J. & Wickens, M. CPEB proteins control two key steps in spermatogenesis in *C. elegans*. *Genes Dev.* **14**, 2596–2609 (2000).
18. Kraemer, B. *et al.* NANOS-3 and FBF proteins physically interact to control the sperm-oocyte switch in *Caenorhabditis elegans*. *Curr. Biol.* **9**, 1009–1018 (1999).
19. Yigit, E. *et al.* Analysis of the *C. elegans* Argonaute family reveals that distinct Argonautes act sequentially during RNAi. *Cell* **127**, 747–757 (2006).
20. Claycomb, J.M. *et al.* The Argonaute CSR-1 and its 22G-RNA cofactors are required for holocentric chromosome segregation. *Cell* **139**, 123–134 (2009).
21. Rhoads, R.E., Dinkova, T.D. & Korneeva, N.L. Mechanism and regulation of translation in *C. elegans*. in *WormBook* (ed. The *C. elegans* Research Community) doi/10.1895/wormbook.1.63.1 (WormBook, 2006).
22. Lee, M.-H. *et al.* Conserved regulation of MAP kinase expression by PUF RNA-binding proteins. *PLoS Genet.* **3**, e233 (2007).
23. Aoki, K., Moriguchi, H., Yoshioka, T., Okawa, K. & Tabara, H. *In vitro* analyses of the production and activity of secondary small interfering RNAs in *C. elegans*. *EMBO J.* **26**, 5007–5019 (2007).
24. Gu, W. *et al.* Distinct argonaute-mediated 22G-RNA pathways direct genome surveillance in the *C. elegans* germline. *Mol. Cell* **36**, 231–244 (2009).
25. Crittenden, S.L. *et al.* A conserved RNA-binding protein controls germline stem cells in *Caenorhabditis elegans*. *Nature* **417**, 660–663 (2002).
26. Galgano, A. *et al.* Comparative analysis of mRNA targets for human PUF-family proteins suggests extensive interaction with the miRNA regulatory system. *PLoS ONE* **3**, e3164 (2008).
27. Merritt, C., Rasoloson, D., Ko, D. & Seydoux, G. 3′ UTRs are the primary regulators of gene expression in the *C. elegans* germline. *Curr. Biol.* **18**, 1476–1482 (2008).
28. Merritt, C. & Seydoux, G. The Puf RNA-binding proteins FBF-1 and FBF-2 inhibit the expression of synaptonemal complex proteins in germline stem cells. *Development* **137**, 1787–1798 (2010).
29. Kershner, A.M. & Kimble, J. Genome-wide analysis of mRNA targets for *Caenorhabditis elegans* FBF, a conserved stem cell regulator. *Proc. Natl. Acad. Sci. USA* **107**, 3936–3941 (2010).
30. She, X., Xu, X., Fedotov, A., Kelly, W.G. & Maine, E.M. Regulation of heterochromatin assembly on unpaired chromosomes during *Caenorhabditis elegans* meiosis by components of a small RNA-mediated pathway. *PLoS Genet.* **5**, e1000624 (2009).
31. Meister, G. *et al.* Identification of novel argonaute-associated proteins. *Curr. Biol.* **15**, 2149–2155 (2005).
32. Parmeggiani, A. & Sander, G. Properties and regulation of the GTPase activities of elongation factors Tu and G, and of initiation factor 2. *Mol. Cell. Biochem.* **35**, 129–158 (1981).
33. Cool, R.H. & Parmeggiani, A. Substitution of histidine-84 and the GTPase mechanism of elongation factor Tu. *Biochemistry* **30**, 362–366 (1991).
34. Mili, S. & Steitz, J.A. Evidence for reassociation of RNA-binding proteins after cell lysis: implications for the interpretation of immunoprecipitation analyses. *RNA* **10**, 1692–1694 (2004).
35. Wang, X., McLachlan, J., Zamore, P.D. & Hall, T.M.T. Modular recognition of RNA by a human pumilio-homology domain. *Cell* **110**, 501–512 (2002).
36. Zamore, P.D., Williamson, J.R. & Lehmann, R. The Pumilio protein binds RNA through a conserved domain that defines a new class of RNA-binding proteins. *RNA* **3**, 1421–1433 (1997).
37. Fox, M.S. & Reijo Pera, R.A. Male infertility, genetic analysis of the *DAZ* genes on the human Y chromosome and genetic analysis of DNA repair. *Mol. Cell. Endocrinol.* **184**, 41–49 (2001).
38. Sonoda, J. & Wharton, R.P. Recruitment of Nanos to *hunchback* mRNA by Pumilio. *Genes Dev.* **13**, 2704–2712 (1999).
39. Ricci, E.P. *et al.* Activation of a microRNA response in *trans* reveals a new role for poly(A) in translational repression. *Nucleic Acids Res.* **39**, 5215–5231 (2011).
40. Nottrott, S., Simard, M.J. & Richter, J.D. Human let-7a miRNA blocks protein production on actively translating polyribosomes. *Nat. Struct. Mol. Biol.* **13**, 1108–1114 (2006).
41. Ingolia, N.T., Ghaemmaghami, S., Newman, J.R. & Weissman, J.S. Genome-wide analysis *in vivo* of translation with nucleotide resolution using ribosome profiling. *Science* **324**, 218–223 (2009).
42. Beckmann, R. *et al.* Alignment of conduits for the nascent polypeptide chain in the ribosome-Sec61 complex. *Science* **278**, 2123–2126 (1997).
43. Miyoshi, K., Okada, T.N., Siomi, H. & Siomi, M.C. Characterization of the miRNA-RISC loading complex and miRNA-RISC formed in the *Drosophila* miRNA pathway. *RNA* **15**, 1282–1291 (2009).
44. Chakravarty, I., Bagchi, M.K., Roy, R., Banerjee, A.C. & Gupta, N.K. Protein synthesis in rabbit reticulocytes. Purification and properties of an Mr 80,000 polypeptide (Co-eIF-2A80) with Co-eIF-2A activity. *J. Biol. Chem.* **260**, 6945–6949 (1985).
45. Caudy, A.A., Myers, M., Hannon, G.J. & Hammond, S.M. Fragile X-related protein and VIG associate with the RNA interference machinery. *Genes Dev.* **16**, 2491–2496 (2002).
46. Walter, P., Ibrahimi, I. & Blobel, G. Translocation of proteins across the endoplasmic reticulum. I. Signal recognition protein (SRP) binds to *in-vitro*-assembled polysomes synthesizing secretory protein. *J. Cell Biol.* **91**, 545–550 (1981).
47. Wolin, S.L. & Walter, P. Signal recognition particle mediates a transient elongation arrest of preprolactin in reticulocyte lysate. *J. Cell Biol.* **109**, 2617–2622 (1989).
48. Hussey, G.S. *et al.* Identification of an mRNP complex regulating tumorigenesis at the translational elongation step. *Mol. Cell* **41**, 419–431 (2011).

ONLINE METHODS

Additional methods. Strains, plasmids and antibodies are detailed in **Supplementary Methods**. Also contained in **Supplementary Methods** are protocols for northern blotting, electrophoretic mobility shift assays and mass spectrometry.

Protein purification. All GST protein purifications were carried out in cold lysis buffer A (50 mM Tris-HCl, pH 7.5, 250 mM NH_4SO_4, 250 mM NaCl, 1 mM EDTA, 5 mM DTT and 1 mM PMSF, supplemented with Roche Complete Protease Inhibitor Cocktail). Cells were lysed, and cleared lysate was incubated with glutathione-Sepharose (GE Healthcare). Protein was eluted in lysis buffer A with 10 mM reduced glutathione. When necessary, GST tags were removed with 1 U PreScission Protease (GE Healthcare).

His_6–CSR-1 was purified as above with minor modifications. Rather than lysis buffer A, lysis buffer B (50 mM NaH_2PO_4, pH 7.4, 10% (v/v) glycerol, 250 mM NH_4SO_4, 250 mM NaCl, 1 mM DTT and 1 mM PMSF, supplemented with Roche Complete Protease Inhibitor Cocktail) was used. Samples were selected with Ni^{2+}–NTA Agarose (Qiagen) and eluted in lysis buffer B with 250 mM imidazole.

Immunoprecipitation and transient transfection. Lysates from transgenic lines expressing GFP::FBF-1 and GFP::tubulin were prepared as above. Cleared lysates were treated with anti-GFP immunoprecipitation with or without RNase A. Coimmunoprecipitated proteins were analyzed by western blotting.

HEK293T cells were transfected using Lipofectamine 2000 (Invitrogen), according to the manufacturer's instructions. Cells were then treated with 0.3% (v/v) formaldehyde and quenched with 0.125 M glycine. RIPA buffer was added (50 mM Tris-HCl, pH 8.0, 150 mM NaCl, 1% (v/v) NP-40, 0.5% (w/v) sodium deoxycholate, 0.1% (w/v) SDS, 2 mM EDTA, 0.5 µg RNase A). Samples were immunoprecipitated with anti-HA antibody, washed in lysis buffer and analyzed by western blotting.

Immunofluorescence and fluorescence microscopy. Adult hermaphrodite gonads were extruded in M9 buffer (with 0.1% (v/v) Tween-20 and 0.25 mM levamisole). Gonads were washed in PBSTw (PBS with 0.1% (v/v) Tween-20) and fixed in 3% (v/v) paraformaldehyde, dissolved in 100 mM K_2HPO_4 (pH 7.2). Samples were washed in PBSTw, and ice-cold methanol was added. Samples were then blocked for 30 min at 22 °C in PBSTw plus 0.5% (w/v) BSA. Primary antibodies (anti–CSR-1 at 1:100, anti–GLD-1 at 1:100 or anti–CYE-1 at 1:300) were added. Samples were washed with PBSTw plus 0.5% (w/v) BSA and incubated with the appropriate secondary antibodies (1:500 dilution), with DAPI. Samples were washed in PBSTw plus 0.5% (w/v) BSA and mounted with Vectashield (Vector Laboratories). Visualization was on a Zeiss LSM 510 Meta confocal microscope. GFP::H2B was visualized as above, but without antibody treatments. DAPI staining was carried out. Samples were examined on an Axio Imager D.1.

RNAi. To conduct RNA interference, L4 hermaphrodite feeding was done. Briefly, the *unc-119(ed3); axIs1723[pie-1* prom:GFP::H2B:*gld-1* 3′UTR*]* and *unc-119(ed3); axIs1775[pie-1* prom:GFP::H2B:*gld-1* mutant 3′UTR*]* strains were picked to RNAi plates. Control plates contained the *Escherichia coli* strain HT115. Only sterile animals (because *csr-1, drh-3, ego-1* and *ekl-1* all result in sterility) were stained with DAPI and scored.

Evolutionary trace and sequence alignment. Conserved sites were identified using evolutionary trace analysis[49]. Protein sequences were aligned to human Pum1 with ClustalW (http://mammoth.bcm.tmc.edu/ETserver.html). Heatmaps depicting normalized conservation Z-scores were generated using Matlab (Mathworks). Conserved residues were visualized on the basis of the structure of human Pum1 (ref. 50).

Protein binding assays. Either 500 ng each of GST–FBF-1, GST–FBF-1(F344R), pETDuet-expressed GST–FBF-1–CSR-1 complex or GST–FBF-1(F344R)–CSR-1 complex were added to 500 ng purified EFT-3 in 20 µL of PBSTw supplemented with 1 mM DTT. Reaction mixtures were incubated with or without 0.5 mM GTP. Reaction mixtures were then added to glutathione-Sepharose, incubated and washed. Equivalent amounts of input proteins and pellets were analyzed. GST-PUM2 binding assays were carried out by adding 50 ng of purified, recombinant protein to 20 µL of reticulocyte lysate. Reaction mixtures were incubated with RNase A (10 µg ml^{-1}), diluted with PBSTw and added to glutathione-Sepharose. Samples were washed with PBSTw, and bound proteins were western blotted as indicated.

GTPase assay. 50 ng each of EFT-3, EFT-3(H95L), GST–FBF-1–EFT-3, GST–FBF-1–CSR-1–EFT-3, or GST–FBF-1(F344R)–CSR-1 with EFT-3 were incubated with 5 µCi [γ-^{32}P]GTP per 50 fmol GTP. Reaction experiments were carried out in GTPase buffer (50 mM MES/KOH, pH 7.5, 150 mM NH_4Cl, 50 mM KCl and 20 mM $MgCl_2$). Three 5-µL aliquots were quantitated. To these aliquots were added 40 µL of 1 M perchloric acid, 20 µL of 0.25 M imidazole (pH 5 with HCl) and 100 µL of 1.5% (w/v) $NaMoO_4$. Phosphomolybdic acid was extracted in butyl acetate and scintillation-counted.

***In vitro* translation.** *In vitro* transcription reaction mixtures were treated with T7 RNA polymerase with the mRNA cap analog m^7G5′ppp5′G (New England Biolabs). For ribosomal footprinting analysis, *in vitro* transcriptions were carried out with [α-^{32}P]UTP.

250 ng GST, GST-PUM2, GST-PUM2(ABD), GST-PUM2(EBD) and GST-PUM2(RBD) were added to 20 µL nuclease-treated, rabbit reticulocyte lysate (Promega). 1 µg nonadenylated or 1 µg polyadenylated firefly luciferase 3× PBEs mRNA was added, as was an amino acid mixture (Promega) and 100 ng control *Renilla* luciferase mRNA. After the reaction, three 5-µL aliquots were quantitated using the Dual Luciferase assay system (Promega). Samples were averaged, and s.d. are from three biological replicates.

Polyribosome analysis. *In vitro* translation reaction mixtures were treated as above, and reactions were quenched with either cycloheximide or puromycin. Reaction mixtures were then separated over a 10–50% linear sucrose gradient. Fractions were collected in 500 µL aliquots and used for northern blotting.

Pulse-chase analysis. *In vitro* translation reaction mixtures were treated as above with modification. Reaction mixtures were pre-incubated, and then m^7G5′ppp5′G (New England Biolabs) was added to a concentration of 2 mM. Immediately, aliquots were removed over the time course.

Ribosome footprinting. *In vitro* translation reaction mixtures were prepared as above; however, only radiolabeled firefly luciferase mRNA was included. Reaction mixtures were quenched with cycloheximide. Samples were then treated with RNase One (Ambion). 2.5 µL were removed (Input RNA) before the remaining samples were separated over a sucrose gradient. RNA was extracted from monoribosome fractions and hybridized to a DNA oligonucleotide array. Samples were compared to input RNA. Hybridization was for 16 h at 45 °C with a wash in 2× and 0.5× SSC for 15 min at 22 °C. Error bars indicate s.d. between three biological replicates.

49. Rajagopalan, L., Pereira, F.A., Lichtarge, O. & Brownell, W.E. Identification of functionally important residues/domains in membrane proteins using an evolutionary approach coupled with systematic mutational analysis. *Methods Mol. Biol.* **493**, 287–297 (2009).
50. Gupta, Y.K., Nair, D.T., Wharton, R.P. & Aggarwal, A.K. Structures of human Pumilio with noncognate RNAs reveal molecular mechanisms for binding promiscuity. *Structure* **16**, 549–557 (2008).

doi:10.1038/nsmb.2214